Composite Structures 286 (2022) 115287

Contents lists available at ScienceDirect

Composite Structures

journal homepage: www.elsevier.com/locate/compstruct

The effect of steady and cyclic environmental conditions on the tensile behaviour of a structural adhesive under sustained loading

Javier Gómez, Cristina Barris *, Younes Jahani, Marta Baena, Lluís Torres

AMADE, Polytechnic School, University of Girona, 17003 Girona, Spain

ARTICLE INFO

Keywords:
Epoxy adhesive
Creep behaviour
High-temperature properties
Thermal analysis
Mechanical testing

ABSTRACT

Structural adhesives are commonly used to bond Fibre Reinforced Polymer (FRP) materials to Reinforced Concrete (RC) structures so they can withstand service conditions. This paper presents an experimental study on the combined effect of sustained loading and service steady and cyclic temperatures on the thermophysical and mechanical properties of an epoxy adhesive.

Four experimental series consisting of nine adhesive tensile dog-bone specimens were tested under sustained loading and temperatures ranging between 18 °C and 43 °C for a duration of 1000 h. Moreover, the residual properties of the adhesive have been evaluated through instantaneous tensile tests and Differential Scanning Calorimetry (DSC) after sustained loading tests.

Results showed a significant increase in strain with time, a reduction in the mechanical properties, and an increase in the glass transition temperature and curing degree of the adhesive after the exposure at service conditions and sustained loading.

From this work it could be concluded that the combination of sustained loading and service temperatures have a significant effect on the creep behaviour of the adhesive, and cyclic temperatures have a greater effect on the adhesive even though the average temperature is below the steady temperature.

1. Introduction

The use of adhesives in civil structures is an excellent solution to bond Fibre Reinforced-Polymers (FRP) to concrete elements [1–4]. Externally Bonded Reinforcement (EBR) [5–8] and Near Surface-Mounted (NSM) [9–12] have become the most prevalent strengthening techniques in this field. In both cases, cold-curing adhesives are the most widely used bonding agents thanks to their ease of use and good mechanical properties after a short curing time. Because the role that structural adhesives play is essential for the adequacy and durability of a concrete-FRP joint, their mechanical properties and effect on the behaviour of bonded joints has been widely studied [13–18]. These studies concluded that the properties of an adhesive directly affect the load carrying capacity and failure mode of the bonded joint.

In real service conditions, along with sustained loading, structural adhesives can be subjected to harmful environmental conditions, which can change their mechanical properties and the durability of the concrete-FRP joint. Therefore, it is extremely important to study how these external actions change the behaviour of structural adhesives. To investigate the mechanical behaviour of a structural adhesive under different environmental conditions, Emara et al. [19] performed an experimental programme combining service temperatures, degrees of humidity and sustained loading levels. Their study concluded that the combination of high service temperature and sustained loading had an important effect on the tensile creep behaviour of the adhesive, whereas relative humidity had a lower effect on the adhesive's performance. Ferrier et al. [17], in turn, found that the service temperature of the adhesive should be around 15 °C lower than the glass transition temperature (T_g) in order to avoid significant creep effects. Other studies have focussed on the mechanical and physical properties of structural adhesives after exposure to different environmental conditions. Hence, Silva et al. [20,21] carried out an experimental programme on dog-bone tensile tests of adhesive specimens after exposing them to different environmental conditions during 120, 240 and 480 days. Their study concluded that specimens exposed to water with chlorides and freeze–thaw cycles experimented a decrease in the T_g, while specimens under thermal cycles experimented an increase in the tensile strength, elastic modulus and T_g, caused by the post-curing effect of the resin. The post-

* Corresponding author.
E-mail address: cristina.barris@udg.edu (C. Barris).

https://doi.org/10.1016/j.compstruct.2022.115287
Received 24 March 2021; Accepted 22 January 2022
Available online 29 January 2022

curing effect on structural adhesives due to environmental conditions was also investigated by Moussa et al. [22,23]. In their studies, dog-bone adhesive specimens were submitted to cyclic temperatures ranging from 30 °C to 60 °C during an exposure time of 14 h that resulted in an increase in the mechanical properties due to post-curing effect on the adhesive. According to [22], the more thermal energy transmitted to the adhesive due to the increment of temperature, the greater the number of molecular links, therefore causing an increase in the adhesive's strength, curing degree (α) and T_g.

The mechanical behaviour of structural adhesives under sustained loading has also been studied from analytical and numerical points of view [18,24–27]. The evolution of the mechanical properties of adhesives is defined by analytical expressions that are based on rheological models and adjusted from experimental results.

Most of the previous studies focussed on constant service conditions. However, less attention has been paid to the study of cycles of temperature, which may be more representative of real-life conditions, where civil structures are subjected to cyclic temperature conditions due to the day-night cycle. In particular, the combined effect of sustained loading and cyclic thermal conditions has been studied for CFRP-steel joints [28–30] and FRP-concrete joints [31–39], but there is still a lack of knowledge on how cyclic environmental conditions specifically affect the mechanical behaviour of the adhesive with time.

The present study aims to contribute to the understanding of the effect of cyclic service temperature conditions on epoxy adhesives for structural strengthening of RC structures through sustained loading tensile tests. Four experimental series studying two steady service temperatures and three cyclic temperatures were carried out, giving a total of 52 specimens. After the tensile sustained loading tests, instantaneous tensile tests were carried out to obtain the residual strength and elastic modulus of the studied adhesive. Finally, Differential Scanning Calorimetry (DSC) analyses were performed to study the influence of steady and cyclic service conditions on the adhesive thermophysical properties.

2. Instantaneous characterization of the adhesive

The adhesive used was the bi-component thixotropic epoxy resin Sika 30. The components were mixed with a resin-hardener ratio of 3:1 at ambient temperature and cured for 12 days. Since this adhesive is commonly used to bond FRP laminates or steel plates to concrete, it is composed of (approximately) 55% silica quartz filler, which provides a high elastic modulus in comparison with other epoxy resins. According to the manufacturer, for a curing time of 7 days under +15 °C, the tensile strength and elastic modulus of the epoxy resin are 26 MPa and 11.2 GPa, respectively.

2.1. Mechanical characterization

The tensile strength and the elastic modulus were obtained from the instantaneous tests of six dog-bone specimens following ISO 527-2 specifications [40]. The tests were performed in an MTS Insight 5 kN testing machine at a test speed of 1 mm/min (Fig. 1). The instrumentation consisted of two strain gauges bonded at each side of the mid-section of the specimen and one extensometer to measure the evolution of strain during the test.

A tensile strength (f_t) of 26.1 MPa (with a Standard Deviation, SD, of 4.5 MPa), an elastic modulus (E_a) of 10.7 GPa (with an SD of 471.4 MPa) and a maximum strain (ε_u) of 2770 με (with an SD of 711 με) were obtained.

2.2. Thermophysical characterization

DSC and Dynamic Mechanical Analysis (DMA) tests were performed after 12 days of curing at 20 °C [41]. The DSC method is used to measure the physical and chemical changes in the material when an increase of temperature is applied to the specimen. During the curing process, the specimen releases energy in an exothermal process, causing a decrease in the enthalpy of reaction. The enthalpy of reaction is measured by integrating the area between the peak corresponding to the curing and a baseline, as is shown in Fig. 2a. The curing degree α is defined as:

$$\alpha = \frac{H_{r,t=0} - H_r}{H_{r,t=0}} \quad (1)$$

where H_r is the enthalpy of reaction in J/g and $H_{r,t=0}$ is the residual enthalpy at curing time $t = 0$ h. Moreover, from the DSC test, the T_g can be obtained according to [41,42].

On the other hand, the DMA test consists of applying a cyclic non-destructive stress to the adhesive specimen at a constant frequency and an increasing temperature with time. This test measures the T_g through three different methods: the storage modulus (E'), the loss modulus (E'') and the loss factor (tan(δ)). The storage modulus is defined as the elastic part of the viscoelastic behaviour of the material and is the material's capacity to store energy. The loss modulus is defined as the viscous part of the viscoelastic behaviour of the material and represents the loss of energy during one loading cycle. The loss factor, or damping, is calculated as the ratio between E'' and E' [43]. The temperatures tested in the DMA ranged between 20 °C and 100 °C with a heating rate of 2 °C/min. A cyclic displacement of 10 μm at a frequency of 1 Hz was applied to the specimen [43].

Fig. 2a and b shows the results obtained from the DSC and the DMA, respectively.

From the DSC tests, T_g was 53.1 °C, the enthalpy of reaction at $t = 0$ h was $H_{r,t=0} = 88.76$ J/g, and the enthalpy at $t = 12$ days was $H_r = 3.29$ J/g, giving $\alpha = 96.3\%$. From the DMA test, the T_g calculated from the onset of the storage modulus curve drop, the loss modulus peak and loss factor peak (tan(δ)) was 53.7 °C, 50.8 °C and 57.5 °C, respectively.

Fig. 1. Set-up for the instantaneous tensile test of adhesive specimens.

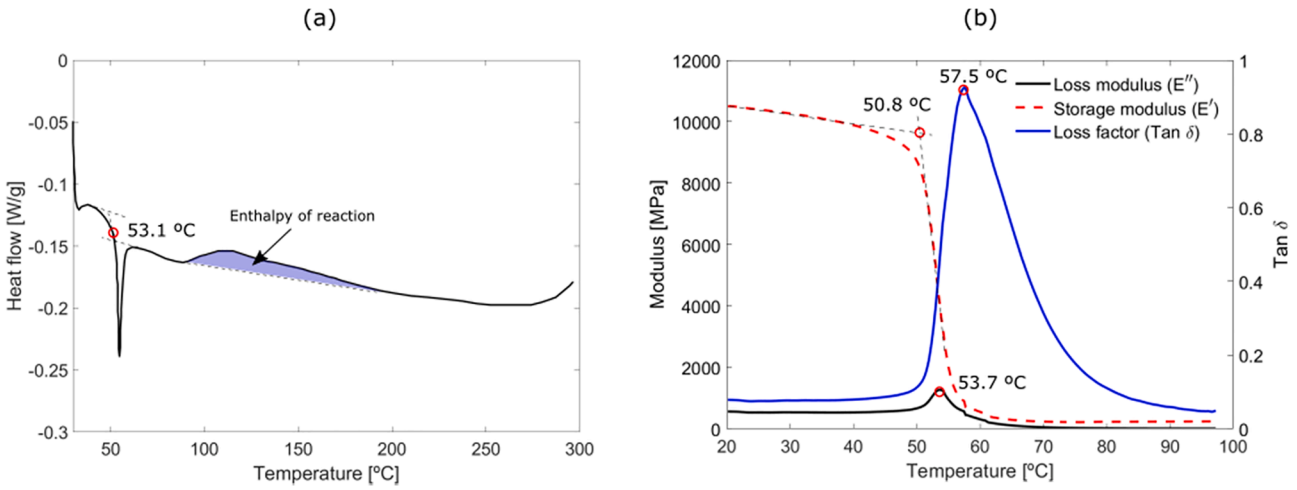

Fig. 2. Results from the (a) DSC test and the (b) DMA test.

3. Experimental time-dependent behaviour of the adhesive

An experimental programme consisting of four experimental series was performed under sustained loading and different temperature conditions and a relative humidity of 55% inside a climatic chamber. Sustained loading was applied through a gravity loading system with a lever arm with a magnification factor of 4 (Fig. 3). The instrumentation consisted of two strain gauges, each one bonded at one side of the mid-section.

Adhesive specimens were named C-%f_t, where C stands for the experimental series and %f_t indicates the percentage of tensile strength (f_t) applied as sustained loading (Table 1).

For each of the four series, three sustained loading levels were tested, corresponding to 15%, 30% and 50% of f_t. Additionally, in one of the experimental series, supplementary levels of 5%, 10%, 20% and 40% of f_t were tested. At each load level, three specimens were tested and one reference specimen (R) was left unloaded, giving a total of 52 adhesive specimens.

Series C1 and C2 were performed at steady temperatures of 20 °C and 40 °C, respectively, while series C3-A, C3-B and C4 were executed in different temperature cycles, as detailed in Table 1. The maximum average service temperature was set to be around 15 °C lower than T_g for all series [17].

In all series except for C4, a seven-day preconditioning stage coincident with the temperature function of the sustained loading test was applied in order to acclimatize the specimens. In series C4, specimens were loaded at the same time as the initiation of the temperature cycles in order to study the effect of preconditioning. Moreover, in C4 the temperature function was triangular, meaning that the objective temperature was steadily increasing or decreasing (see Fig. 4), without any horizontal plateau.

For series C3, two different phases were applied. In phase A (C3-A), a range of temperatures very similar to those of C4 (18–38 °C, compared to 20–40 °C in C4), but with a trapezoidal temperature cycle were applied (see Fig. 4). This phase was finalised at 600 h because the amplitude of strain caused by the thermal cycle stabilized. After that, the specimens were subjected to the phase B (C3-B) conditions, where the objective trapezoidal cyclic temperature was increased from 22 °C to 43 °C. After that, to study the behaviour of the specimens under a change on the climatic conditions, the specimens were subjected to the phase B (C3-B) conditions, where the objective trapezoidal cyclic temperature was increased from 22 °C to 43 °C.

Fig. 4 shows the comparison between the temperature measured on the specimens' surface (black curve) and the objective temperature (red curve) of every experimental series under cyclic temperature.

In the C3 series, some differences can be observed between the objective ascending temperature (red line) and the surface temperature of the specimen (black line). This could be attributed to a combined effect between the programmed rate of variation and the thermal inertia of additional materials in the chamber during the test. The softer slope of the ascending branch (in °C/min) in the cycles of series C4 compared to C3 allowed the specimens to more precisely follow objective cycle.

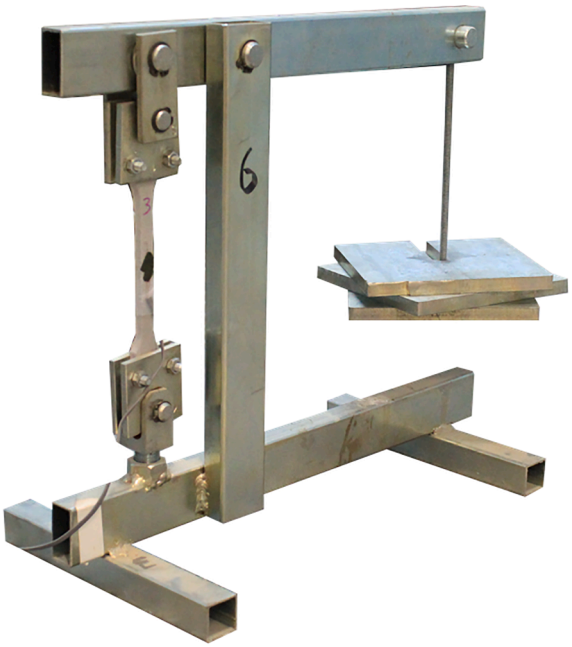

Fig. 3. Set-up of the sustained loading test.

3.1. Evolution of strain with time

Fig. 5 presents the evolution of axial strain in the adhesive specimens at the different sustained loading stages (detailed in Table 1) for each series. Each curve was obtained as the average of the three specimens tested at the given sustained loading level. In Fig. 5c, the dashed grey line indicates the end of the test, while black crosses in Fig. 5b, d and e indicate the failure of the specimens.

Regardless of the temperature conditioning (steady or cyclic temperature), an initial stage with a high increase of strain and a second stage where the increase of strain tends to be lower and more constant

Table 1
Experimental series.

Series	Load level [% of P_u] (no of specimens)	Temperature function [24 h]	Preconditioning	Phase	Specimens' surface temperature [°C]	Average temperature of the specimen' surface [°C]	Test duration [hours]
C1	15 (3)/30 (3)/50 (3)/R (1)	Steady	Yes	–	20	20	1000
C2	5 (3)/10 (3)/15 (3)/20 (3)/30 (3)/40 (3)/50 (3)/R (1)	Steady	Yes	–	40	40	1000
C3	15 (3)/30 (3)/50 (3)/R (1)	Trapezoidal	Yes	A	18–37	26.9	600
				B	23–43	33.7	1000
C4	15 (3)/30 (3)/50 (3)/R (1)	Triangular	No	–	20–40	30.0	1000

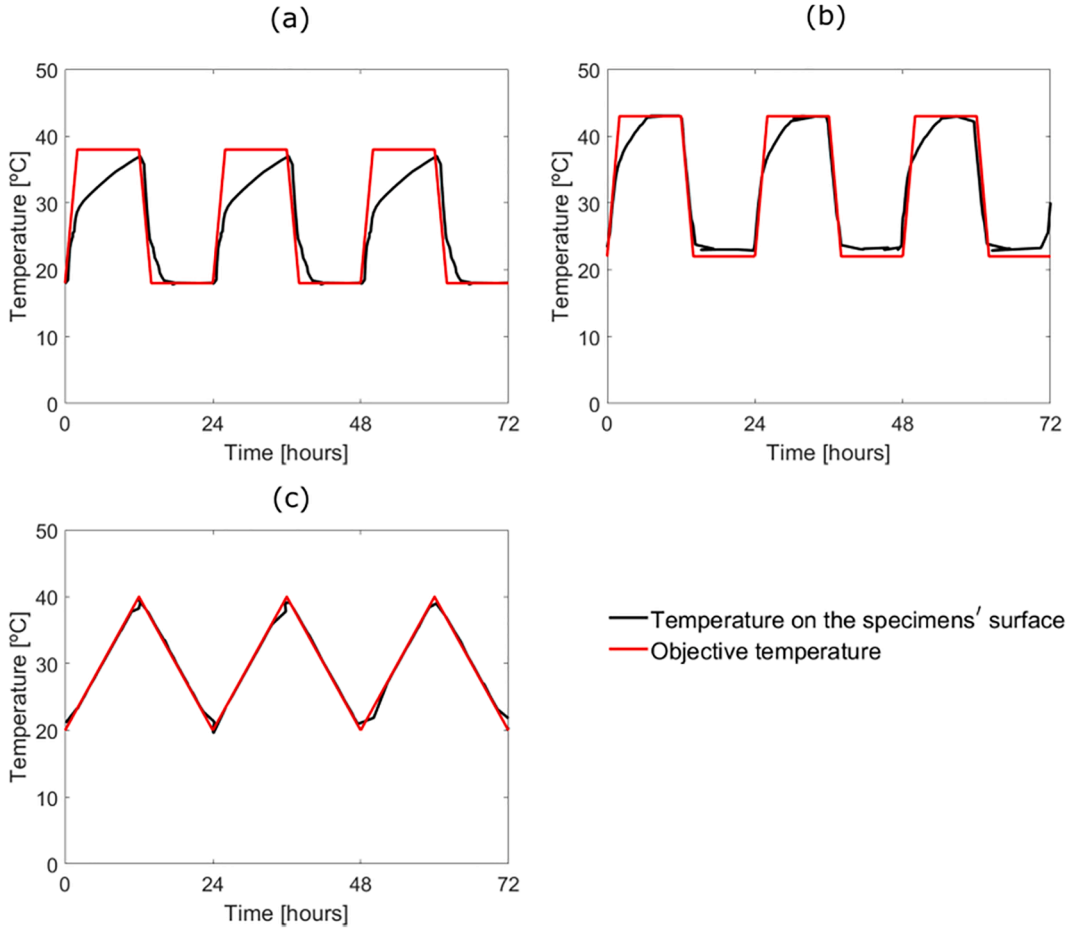

Fig. 4. Temperature cycles applied in the experimental series (a) C3-A, (b) C3-B and (c) C4.

can be observed. Some specimens eventually experienced a high increase of strain that led to failure. In the following sub-sections, the effect of sustained loading, high service temperature, preconditioning and thermal cycles is further analysed and discussed.

3.1.1. *Effect of sustained loading*

The increase in sustained loading causes a general increment of the time-dependent strain, as expected. Furthermore, specimens under 15% of f_t did not fail during the test, even though specimens C4-15 developed a significant increment of strain during the first temperature cycle due to the lack of preconditioning. For sustained loading levels of 30% of f_t, only specimens C4-30, failed after a few hours of loading. Finally, for specimens loaded at 50% of f_t, only C1 and C3-A specimens endured until the end of the test, developing a final strain of 3120 $\mu\varepsilon$ and 5345 $\mu\varepsilon$ for C1 and C3-A, respectively. In contrast, C2, C3-B and C4 specimens under 50% of f_t failed after 11 h, 197 h and 7 h, respectively.

In some specimens, the time-dependent strain was higher than the instantaneous ultimate strain. This effect was also observed in [19,26]. Costa et al. [26] attributed this phenomenon to a continuous reorganization of the internal structure of the adhesive, allowing it to withstand higher deformations than the ultimate strain under instantaneous load.

3.1.2. *Effect of high service temperature*

The strain level increased with the increase in temperature (C2 series in Fig. 5b compared to C1 series in Fig. 5a). Furthermore, specimens under 40 °C experimented the highest strain with time of all the experimental series, which is because the average temperature during the test was also the highest [19,44]. In this series, no failure was obtained in specimens under sustained loading levels up to 40% of f_t.

3.1.3. *Effect of the preconditioning period*

A preconditioning stage of seven days was applied to all the experimental series except series C4, where significatively higher strains were observed in their first thermal cycle in comparison with the others. Furthermore, C4 specimens failed after 12 h (when the first peak temperature of 40 °C was achieved), and 7 h (when the temperature was

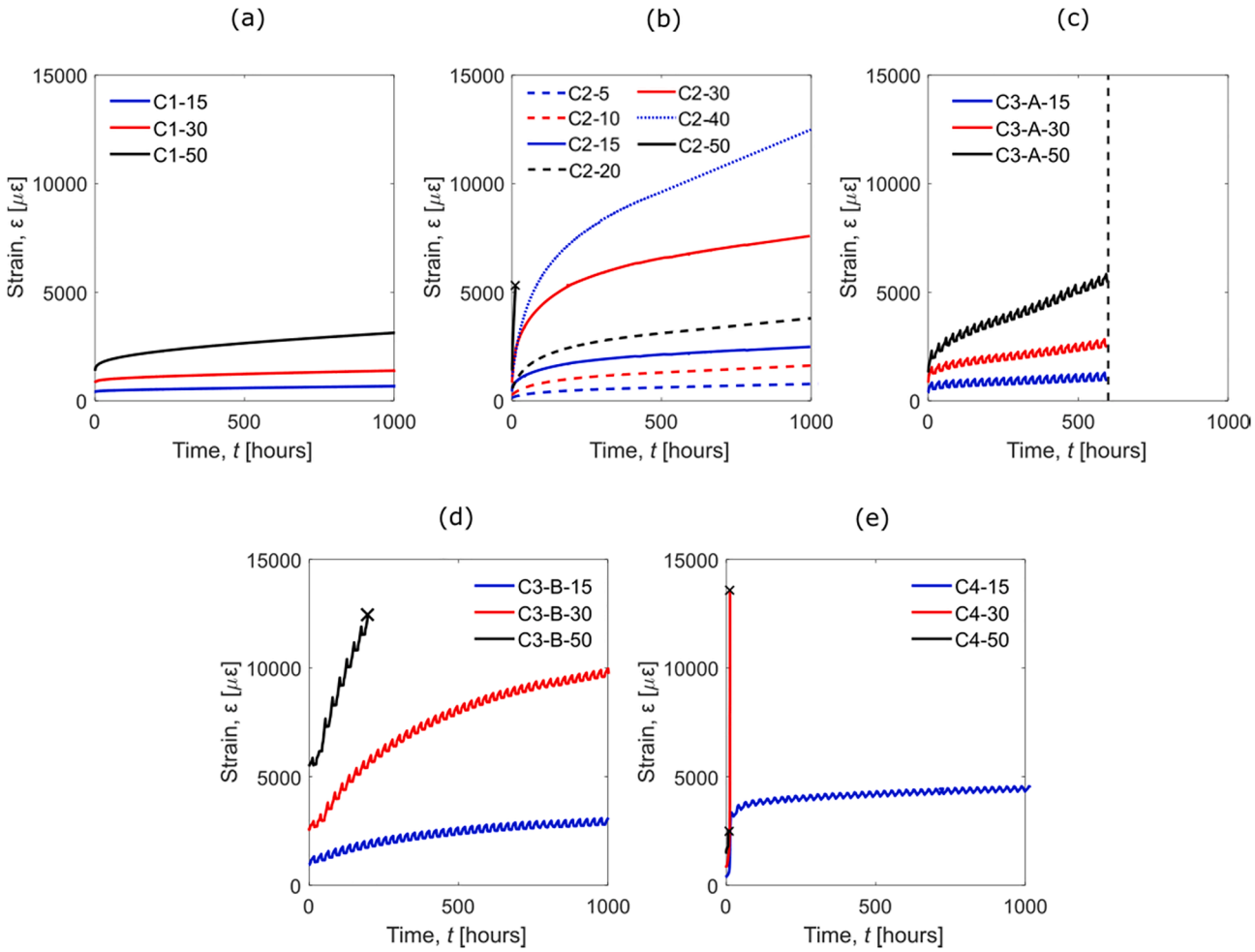

Fig. 5. Evolution of strain obtained in experimental series (a) C1, (b) C2, (c) C3-A, (d) C3-B and (e) C4.

22.7 °C) for loading levels of 30% and 50% of f_t, respectively.

3.1.4. Effect of thermal cycles on the overall time-dependent behaviour

The effect of temperature cycles on the evolution of the tensile strain can be identified in series C3 and C4 (Fig. 5c, d and e) through relatively small oscillations of strain at every cycle. The amplitude of strain related to temperature cycles, caused by the thermal expansion and contraction of the adhesive, was observed not to be significant compared to the mean value of the time-dependent strain, especially in the stage where creep tends to a constant slope. However, to better identify the effect of

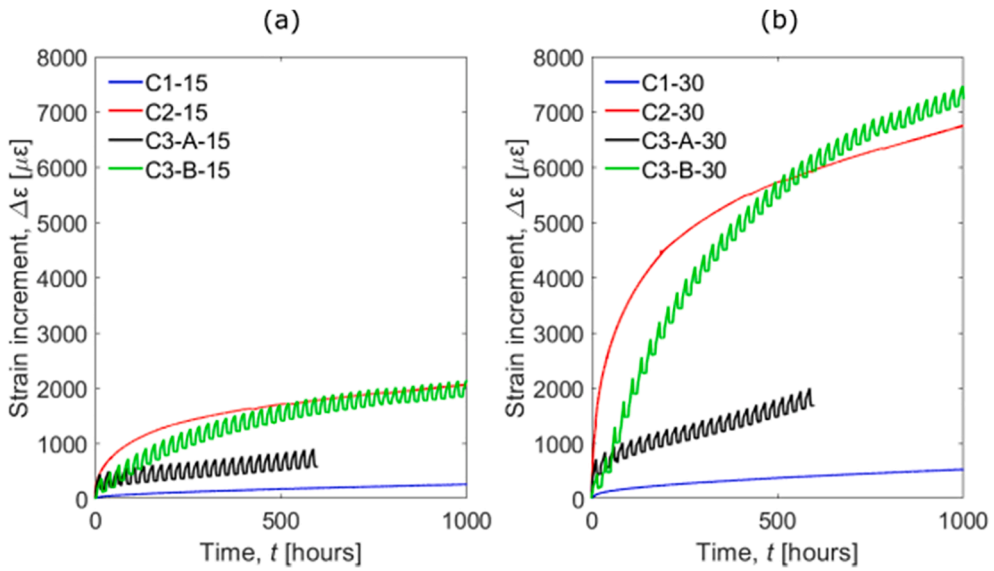

Fig. 6. Increment of strain with time for specimens under (a) 15% of f_t and (b) 30% of f_t.

thermal cycles on the time-dependent strain behaviour, Fig. 6 represents the increment of adhesive strain with time occurring after instantaneous deformation ($\Delta\varepsilon$) for experimental series C1, C2, C3-A and C3-B, at the loading levels of 15 and 30% of f_t.

It is observed that the strain response of series C3-A (cyclic temperature between 18 °C and 37 °C with average value of 26.9 °C) lies between that of the C1 and C2 series (steady temperature conditions, at 20 °C and 40 °C, respectively), as was to be expected.

However, for the case of C3-B (cyclic temperature between 23 °C and 43 °C with an average value of 33.7 °C), the mean time-dependent strain clearly surpassed the trend indicated by the C2 series in specimens under 30% of f_t (C3-B-30) at $t = 540$ h and at around 1000 h the C3-B-15 specimens reached the C2 trend. Even though the average temperature in C3-B was lower than the steady temperature in C2, the fact that the maximum temperature of the C3-B series was higher than 40 °C, might have caused more molecular motion which degraded the secondary bonds of the adhesive thus increasing the strain in the specimen [22] and, consequently, increasing the creep behaviour of the adhesive. Furthermore, it should be remembered that the C3-B series was previously loaded under C3-A thermal conditions for 600 h, hence, the initial stage with high creep deformation due to loading had already taken place during the C3-A thermal period. The fact that during the stage with a rather constant slope the C3-B specimens showed higher value of$\Delta\varepsilon$, might indicate that the temperature cycles caused greater damage to the specimens (measured as strain increment in this work).

3.1.5. *Effect of the thermal cycles on the strain amplitude*

To further study the effects of sustained loading on strain oscillations caused by the thermal cycles, the evolution of ascending amplitude of strain ($A_{\varepsilon,a}$) and the descending amplitude of strain ($A_{\varepsilon,d}$) at each cycle was measured. $A_{\varepsilon,a}$ and $A_{\varepsilon,d}$ were calculated as the strain difference between the lower and upper temperatures at each thermal cycle (valley to peak for the ascending amplitude and peak to valley for the descending one). Results are presented in Fig. 7 for experimental series C3-A, C3-B and C4.

In general, for sustained loadings of 30% and 50% of f_t, the ascending amplitude is higher than the descending one, due to the effect of creep on the adhesive. This effect cannot be noticed in specimens loaded at 15% of f_t, probably because, in this case, the effect of creep is not so relevant.

Furthermore, the difference between $A_{\varepsilon,a}$ and $A_{\varepsilon,d}$ decreases with time which might be attributed to the stabilizations of the creep effect in its secondary stage. However, for the case of specimens C3-A-50, loaded at 50% of f_t, the difference between $A_{\varepsilon,a}$ and $A_{\varepsilon,d}$ is maintained until the end of the test, showing that for higher load levels, creep effects play an important role on the strain behaviour.

Regarding the effect of preconditioning (Fig. 7c), as was previously observed in Fig. 5e, high oscillations of strain were obtained during the initial thermal cycles. In particular, C4-15 specimens experimented an $A_{\varepsilon,a} = 2890$ με. This value has not been included in Fig. 7c for scaling reasons. Beyond the second thermal cycle, the specimens were better conditioned and the amplitude of strain decreased, obtaining a lower amplitude of strain in comparison to C3-A and C3-B.

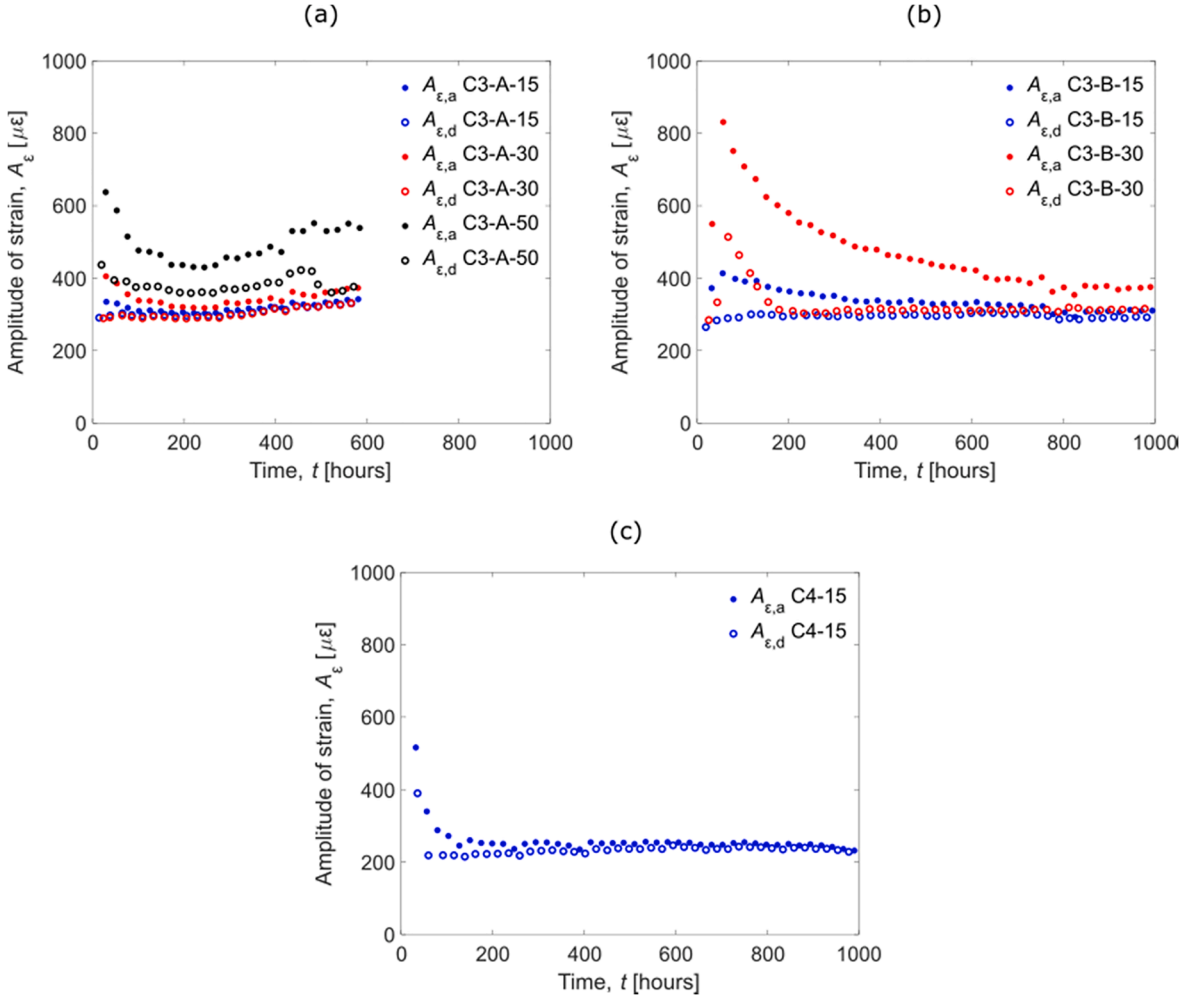

Fig. 7. Evolution of the strain amplitude obtained in the adhesive specimens in experimental series (a) C3-A, (b) C3-B and (c) C4.

3.2. Evolution of creep compliance with time

Creep compliance, $J(t)$, provides information about the linearity of the viscoelastic behaviour of adhesive with respect to the load applied. $J(t)$ was obtained by dividing the adhesive tensile strain $\varepsilon(t)$ by the applied stress σ_0 [45]:

$$J_C(t) = \frac{\varepsilon(t)}{\sigma_0} \tag{2}$$

Fig. 8 presents the creep compliance curves for each experimental series. Continuous blue, red and black curves stand for specimens under 15%, 30% and 50% of f_t, respectively. Additionally, for the C2 series, dashed blue, red, and black curves represent specimens under 5%, 10% and 20% of f_t and the dotted blue line represent specimens under 40% of f_t.

In the C1 series, similar creep compliance values were obtained for specimens under 15% and 30% of f_t, while it was slightly higher for the C1-50 specimens, indicating a linear viscoelastic behaviour for specimens at room temperature conditions until sustained loading levels up to 30% of f_t.

As the service temperature increased, higher values of creep compliance were obtained. For example, in the C2 series, specimens under 30% of f_t showed a J_c ($t = 1000$ h) value of 1047 MPa^{-1}, compared to 184.5 MPa^{-1}, obtained in C1. Furthermore, it was also observed that for the C2 series similar curves were obtained for sustained loading levels ranging between 5% and 15% of f_t. For higher sustained loading levels, higher creep compliance curves were obtained, meaning that the linear viscoelastic behaviour can be assumed for sustained loading levels up to 15% of f_t. By comparing the C2 series with C1, it can be seen that the maximum loading level that can be included in the viscoelastic behaviour decreases as service temperatures increases.

In the experimental series C3-A, where cyclic temperature conditions were applied, slightly different creep compliance curves were obtained for all load levels. Although small but some difference is appreciated between specimens loaded at loaded at 15% and 30% when compared to C1. Moreover, from comparison between C3-A and C3-B series, it can be seen that as the average service temperature increased, higher values of creep compliance were obtained, as expected.

In the non-preconditioned series C4, the increase in temperature during the first cycles caused high values of strain to develop in the adhesive and, consequently, high values of creep compliance were obtained.

4. Post-long-term mechanical and thermophysical behaviour of the adhesive specimens

To study the effect of high service temperatures and sustained loading on the mechanical and thermophysical properties, tensile tests and DSC tests were performed in each experimental series after the sustained loading tests.

For the experimental series C3-A, before C3-B series started, one adhesive specimen under 15% f_t was maintained at room conditions (20 ± 1 °C) to study the post-long-term behaviour. Moreover, to study the effects of the temperature cycles on the adhesive's response, one

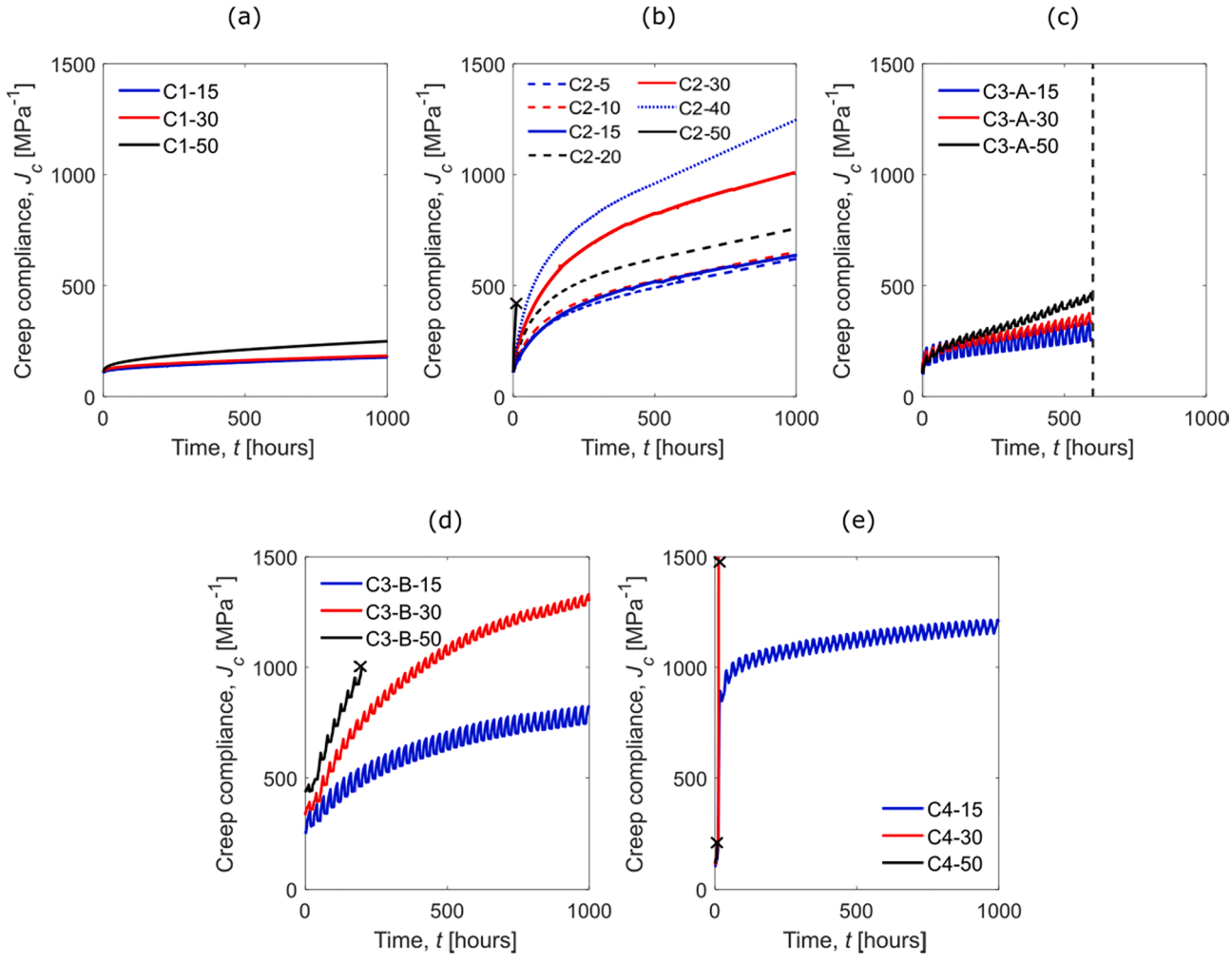

Fig. 8. Creep compliance curves obtained in experimental series (a) C1, (b) C2, (c) C3-A, (d) C3-B and (e) C4.

specimen was kept inside the climatic chamber without sustained loading during the experimental series C3-A and C3-B.

4.1. Results from the mechanical characterization

Tensile tests until failure were performed for all specimens that did not fail during the sustained loading tests to study the effect of sustained loading and service conditions on the load carrying capacity of adhesive.

Table 2 shows the mechanical properties obtained from the post-sustained instantaneous loading tests ($E_{a,LT}$ and $f_{t,LT}$), and the ratio with the instantaneous values previously obtained in Section 2.1 (E_a and f_t).

Overall, all specimens subjected to sustained loading experienced a decrease in the mechanical properties of the adhesive, both in the tensile strength and the elastic modulus. In general, when increasing the level of sustained loading, the mechanical properties decreased. The specimen subjected to thermal conditions but unloaded (C3-B-R-PLT-NL) did not suffer any reduction in their tensile strength that should be taken into account, and kept almost the same elastic modulus (ratios of 1.03 and 0.96 were obtained for E_a and f_t, respectively).

Taking series C1 as a reference, it can be generally observed that specimens from series C2 presented slightly higher $f_{t,LT}$ and lower $E_{a,LT}$. The increase in $f_{t,LT}$ could be explained because of a post-curing effect taking place at high temperatures (always below the T_g), while the reduction of $E_{a,LT}$ could be explained because these specimens underwent longer time-dependent strains once the specimen was unloaded which induced a less stiff response.

Results from the specimens in the C3-A series (cyclic temperature between 18 °C and 37 °C with average value of 26.9 °C) fell between those of the C1 and C2 series. Specimens from series C3-B obtained similar $f_{t,LT}$ as the specimens in C2. Even though the average temperature in series C3-B was lower than temperature in series C2, the maximum temperature of the thermal cycle in C3-B caused a post-curing effect which resulted in a similar value of $f_{t,LT}$.

From the experimental series C4, only specimens under 15% of f_t could be tested. In this case, a substantial decrease in the mechanical properties was observed in the post-long-term tests, which could be attributed to the lack of preconditioning of these specimens.

Table 2
Tensile strength and stiffness of adhesive specimens after long-term tests.

Series	Specimen	$f_{t,LT}$ [MPa]	$\frac{f_{t,LT}}{f_t}$	$E_{a,LT}$ [MPa]	$\frac{E_{a,LT}}{E_a}$
C1	C1-R-PLT-15	21.8 (SD = 1.89)	0.83	9147.5 (SD = 561.3)	0.85
	C1-R-PLT-30	22.5 (SD = 1.55)	0.86	9030.0 (SD = 302.6)	0.84
	C1- R-PLT-50	22.0 (SD = 2.60)	0.84	8815.5 (SD = 344.8)	0.82
C2	C2-R-PLT-15	24.2 (SD = 0.4)	0.92	8907.1 (SD = 555.2)	0.83
	C2-R-PLT-30	22.5 (SD = 1.8)	0.86	7573.0 (SD = 677.1)	0.71
	C2-R-PLT-50	–	–	–	–
C3-A	C3-A-R-PLT-15	23.2	0.88	8984.0	0.84
	C3-A-R-PLT-30	*	*	*	*
	C3-A- R-PLT-50	*	*	*	*
C3-B	C3-B-R-PLT-15	24.1 (SD = 2.65)	0.92	9284.4 (SD = 2106.2)	0.87
	C3-B-R-PLT-30	23.3 (SD = 2.96)	0.89	8521.8 (SD = 1154.3)	0.79
	C3-B-R-PLT-50	–	–	–	–
	C3-B- R-PLT-NL	26.85	1.03	10294.3	0.96
C4	C4-R-PLT-15	20.1 (SD = 1.1)	0.77	7928.9 (SD = 497.7)	0.74
	C4-R-PLT-30	–	–	–	–
	C4- R-PLT-50	–	–	–	–

Note: "–" indicates that the specimen failed during the sustained loading test and "*" indicates that the specimen was not tested post-long-term because it was used in series C3-B.

4.2. Results from thermophysical characterization

Table 3 shows H_r, α and T_g calculated from the DSC tests performed after each experimental series and at the reference time of 12 days (R), previously shown in Section 2.2.

The curing degree α obtained in the C1 series after the sustained loading test was slightly higher than the value obtained in the instantaneous characterization, while no difference in T_g was observed. In the rest of the experimental series, where specimens were subjected to higher temperatures than in C1, the curing degree was higher, indicating some post-curing effect. This increasing effect was also observed in T_g, which increased with the service temperature (C2 compared to C1). Hence, it can be stated that relatively high service temperatures might cause more cross-links to develop between the molecules of the adhesive specimen, thus increasing the glass transition temperature [16,21–23]. Regarding the effect of the temperature cycles, it can be seen that higher T_g values were obtained in comparison with the C2 series, as was observed in Silva et al. [21]. From comparisons between the C3-A and C3-B series, it can be seen that the higher increase of T_g was obtained as higher temperature cycles were applied (C3-B compared to C3-A).

5. Conclusions

The present work aimed to study the behaviour of a structural adhesive under sustained loading and different steady and cyclic temperature service conditions. For that purpose, four experimental series of sustained loading tensile tests were carried out. In each series, nine specimens were subjected to different levels of sustained loading (15%, 30% and 50% of the tensile strength) for 1000 h inside a climatic chamber. The service temperature conditions were modified for each series in order to observe their influence on the tensile response of the adhesive. From the sustained loading tests, the following conclusions can be drawn:

- The tensile strain in the adhesive increased with the service temperature and sustained loading, as would be expected.
- Only specimens from the experimental series C1 (steady temperature at 20 °C) and C3-A (cyclic temperature between 18 °C and 38 °C) were able to withstand a load level of 50% of f_t until the end of the test (1000 h and 600 h, respectively).
- The lack of a preconditioning stage caused high values of strain in the C4 series, leading to premature failure in specimens under 30% and 50% of f_t.
- Higher strains were obtained in comparison with the ultimate instantaneous strain due to the reorganization of the internal structure of the adhesive specimens with time.
- In the experimental C1 series, a linear creep stage could be assumed for sustained loading levels up to 30% of the tensile strength, while in

Table 3
Enthalpy of reaction (H_r), curing degree (α) and glass transition temperature (T_g) obtained from the DSC test after each experimental series.

	Series					
	R	C1	C2	C3-A	C3-B	C4
H_r [J/g]	3.3	3.1	1.7	1.9	0	2.6
α [%]	96.3	96.6	98.0	97.9	100	97.1
T_g [°C]	53.1	53.1	56.7	59.7	65.4	58.9

the experimental C2 series (steady temperature at 40 °C), a linear viscoelastic behaviour was observed for specimens under sustained loading levels between 5% and 15% of f_t.
- Thermal cycles in C3-B caused a higher increase of strain than expected, considering the average temperature of the cycles. Additionally, temperature cycles caused oscillations of strain in the specimens. That said, however, these strain variations were not significant in comparison with the evolution of strain with time.
- The strain amplitude observed in the specimens decreased with time, becoming higher as the sustained load level increased.

Additionally, tensile and DSC tests were performed to study the mechanical and thermophysical properties of the adhesive before and after service conditions. From this, the following conclusions can be stated:

- A general decrease of the mechanical properties was observed in the tensile tests after the sustained loading.
- A general increase in T_g and α was observed after the sustained loading tests. A higher increase in T_g was observed in specimens that were subjected to cyclic temperature (C3-A, C3-B, C4) compared to the series held under steady temperatures (C1 and C2).
- As the average temperature in the experimental series increased, the value of T_g increased as well.

Declaration of Competing Interest

The authors declare that they have no known competing financial interests or personal relationships that could have appeared to influence the work reported in this paper.

Acknowledgements

This work was supported by the Spanish Government (MINECO) [Project Ref. BIA2017-84975-C2-2-P]; the University of Girona [grant IFUdG2018/28 and MOB2019]; and the Generalitat de Catalunya [grant number 2019FI_B 00054]. The authors wish to acknowledge the support of SIKA for supplying the epoxy adhesive used in this study.

References

[1] Blaschko M, Zilch K. Rehabilitation of concrete structures with CFRP strips glued into slits. Mater Struct 1999;26:185–9. https://doi.org/10.1007/BF02472937.
[2] Meier U. Carbon Fiber-Reinforced Polymers : Modern Materials in Bridge Engineering. Struct Eng Int 1992;2:7–12. https://doi.org/10.2749/101686692780617020.
[3] Buyukozturk BO, Bakhoum MM, Member S, Beattie SM. Shear behaviour of joints in precast concrete segmental bridges 1991;116:3380–401.
[4] Tumialan JG, Vatovec M, Kelley PL. Case study: strengthening of parking garage decks with near-surface-mounted CFRP bars. J Compos Constr 2007;11(5):523–30. https://doi.org/10.1061/(ASCE)1090-0268(2007)11:5(523).
[5] Chen JF, Teng JG. Anchorage Strength Models for FRP and Steel Plates. J Struct Eng 2001;127:784–91.
[6] Yuan H, Teng JG, Seracino R, Wu ZS, Yao J. Full-range behavior of FRP-to-concrete bonded joints. Eng Struct 2004;26(5):553–65. https://doi.org/10.1016/j.engstruct.2003.11.006.
[7] Lu XZ, Teng JG, Ye LP, Jiang JJ. Bond-slip models for FRP sheets/plates bonded to concrete. Eng Struct 2005;27(6):920–37. https://doi.org/10.1016/j.engstruct.2005.01.014.
[8] Ferracuti B, Savoia M, Mazzotti C. Interface law for FRP-concrete delamination. Compos Struct 2007;80(4):523–31. https://doi.org/10.1016/j.compstruct.2006.07.001.
[9] De Lorenzis L, Teng JG. Near-surface mounted FRP reinforcement: An emerging technique for strengthening structures. Compos Part B Eng 2007;38(2):119–43.
[10] Seracino R, Jones NM, Ali MS, Page MW, Oehlers DJ. Bond Strength of Near-Surface Mounted FRP Strip-to-Concrete Joints. J Compos Constr 2007;11(4):401–9. https://doi.org/10.1061/(ASCE)1090-0268(2007)11:4(401).
[11] Haskett M, Oehlers DJ, Mohamed Ali MS. Local and global bond characteristics of steel reinforcing bars. Eng Struct 2008;30(2):376–83. https://doi.org/10.1016/j.engstruct.2007.04.007.
[12] Sena Cruz JM, Barros JAO, Gettu R, Azevedo ÁFM. Bond Behavior of Near-Surface Mounted CFRP Laminate Strips under Monotonic and Cyclic Loading. J Compos Constr 2006;10(4):295–303. https://doi.org/10.1061/(ASCE)1090-0268(2006)10:4(295).
[13] Benyoucef S, Tounsi A, Addabedia E, Meftah S. Creep and shrinkage effect on adhesive stresses in RC beams strengthened with composite laminates. Compos Sci Technol 2007;67(6):933–42. https://doi.org/10.1016/j.compscitech.2006.07.007.
[14] Choi K-K, Meshgin P, Reda Taha MM. Shear creep of epoxy at the concrete-FRP interfaces. Compos Part B Eng 2007;38(5-6):772–80.
[15] Torres L, Sharaky IA, Barris C, Baena M. Experimental study of the influence of adhesive properties and bond length on the bond behaviour of NSM FRP bars in concrete. J Civ Eng Manag 2016;22:808–17. https://doi.org/10.3846/13923730.2014.914097.
[16] Benedetti A, Fernandes P, Granja JL, Sena-Cruz J, Azenha M. Influence of temperature on the curing of an epoxy adhesive and its influence on bond behaviour of NSM-CFRP systems. Compos Part B Eng 2016;89:219–29. https://doi.org/10.1016/j.compositesb.2015.11.034.
[17] Ferrier E, Michel L, Jurkiewiez B, Hamelin P. Creep behavior of adhesives used for external FRP strengthening of RC structures. Constr Build Mater 2011;25(2):461–7. https://doi.org/10.1016/j.conbuildmat.2010.01.002.
[18] Ferrier E, Hamelin P. Long-time concrete-composite interface characterization for reliability prediction of RC beam strengthened with FRP. Mater Struct Constr 2002;35:564–72. https://doi.org/10.1617/13691.
[19] Emara M, Torres L, Baena M, Barris C, Moawad M. Effect of sustained loading and environmental conditions on the creep behavior of an epoxy adhesive for concrete structures strengthened with CFRP laminates. Compos Part B Eng 2017;129:88–96. https://doi.org/10.1016/j.compositesb.2017.07.026.
[20] Silva P, Valente T, Azenha M, Sena-Cruz J, Barros J. Viscoelastic response of an epoxy adhesive for construction since its early ages: Experiments and modelling. Compos Part B Eng 2017;116:266–77. https://doi.org/10.1016/j.compositesb.2016.10.047.
[21] Silva P, Fernandes P, Sena-Cruz J, Xavier J, Castro F, Soares D, et al. Effects of different environmental conditions on the mechanical characteristics of a structural epoxy. Compos Part B Eng 2016;88:55–63.
[22] Moussa O, Vassilopoulos AP, De Castro J, Keller T. Time-temperature dependence of thermomechanical recovery of cold-curing structural adhesives. Int J Adhes Adhes 2012;35:94–101. https://doi.org/10.1016/j.ijadhadh.2012.02.005.
[23] Moussa O, Vassilopoulos AP, Castro Jd, Keller T. Long-term development of thermophysical and mechanical properties of cold-curing structural adhesives due to post-curing. J Appl Polym Sci 2013;127(4):2490–6. https://doi.org/10.1002/app.37965.
[24] Meshgin P, Choi K-K, Reda Taha MM. Experimental and analytical investigations of creep of epoxy adhesive at the concrete-FRP interfaces. Int J Adhes Adhes 2009;29(1):56–66. https://doi.org/10.1016/j.ijadhadh.2008.01.003.
[25] Majda P, Skrodzewicz J. A modified creep model of epoxy adhesive at ambient temperature. Int J Adhes Adhes 2009;29(4):396–404. https://doi.org/10.1016/j.ijadhadh.2008.07.010.
[26] Costa I, Barros J. Tensile creep of a structural epoxy adhesive: Experimental and analytical characterization. Int J Adhes Adhes 2015;59:115–24. https://doi.org/10.1016/j.ijadhadh.2015.02.006.
[27] Feng C-W, Keong C-W, Hsueh Y-P, Wang Y-Y, Sue H-J. Modeling of long-term creep behavior of structural epoxy adhesives. Int J Adhes Adhes 2005;25(5):427–36. https://doi.org/10.1016/j.ijadhadh.2004.11.009.
[28] Agarwal A, Ng TS, Foster S, Hamed E. Durability of steel-CFRP adhesive joints under sustained loading and wet thermal-cycles. In: ICCM Int Conf Compos Mater 2013;2013–July:2317–25.
[29] Agarwal A, Foster SJ, Hamed E. Testing of new adhesive and CFRP laminate for steel-CFRP joints under sustained loading and temperature cycles. Compos Part B Eng 2016;99:235–47. https://doi.org/10.1016/j.compositesb.2016.06.039.
[30] Agarwal A, Foster SJ, Hamed E. Wet thermo-mechanical behavior of steel-CFRP joints - An experimental study. Compos Part B Eng 2015;83:284–96. https://doi.org/10.1016/j.compositesb.2015.08.025.
[31] Liang H, Li S, Lu Y, Yang T. The combined effects of wet–dry cycles and sustained load on the bond behavior of FRP–concrete interface. Polym Compos 2019;40(3):1006–17. https://doi.org/10.1002/pc.24785.
[32] Shi J, Zhu H, Wu Z, Seracino R, Wu G. Bond Behavior between Basalt Fiber-Reinforced Polymer Sheet and Concrete Substrate under the Coupled Effects of Freeze-Thaw Cycling and Sustained Load. J Compos Constr 2013;17(4):530–42.
[33] Hartanto D, Hamed E, Agarwal A, Foster SJ. Behaviour of steel-CFRP lap joints under hygrothermal cycles and sustained loadings. Compos Struct 2018;203:740–9. https://doi.org/10.1016/j.compstruct.2018.07.032.
[34] Gullapalli A, Lee JH, Lopez MM, Bakis CE. Sustained Loading and Temperature Response of Fiber-Reinforced Polymer-Concrete Bond. Transp Res Rec J Transp Res Board 2009;2131(1):155–62. https://doi.org/10.3141/2131-15.
[35] Jeong Y, Lopez MM, Bakis CE. Effects of temperature and sustained loading on the mechanical response of CFRP bonded to concrete. Constr Build Mater 2016;124:442–52. https://doi.org/10.1016/j.conbuildmat.2016.07.123.
[36] Jeong Y, Lopez MM, Bakis CE. Effects of Sustained Loading and Temperature on a Concrete-Epoxy Bonded Interface. J Mater Civ Eng 2020;32:1–13. https://doi.org/10.1061/(ASCE)MT.1943-5533.0003051.
[37] Gamage JCPH, Al-Mahaidi R, Wong B, Ariyachandra MREF. Bond characteristics of CFRP-strengthened concrete members subjected to cyclic temperature and mechanical stress at low humidity. Compos Struct 2017;160:1051–9. https://doi.org/10.1016/j.compstruct.2016.10.131.
[38] Gamage JCPH, Al-Mahaidi R, Wong MB. Integrity of CFRP-concrete bond subjected to long-term cyclic temperature and mechanical stress. Compos Struct 2016;149:423–33. https://doi.org/10.1016/j.compstruct.2016.04.040.

[39] Dash S, Jeong Y, Lopez MM, Bakis CE. Experimental Characterization of Moisture, Temperature and Sustained Loading on Concrete-FRP Bond Performance. In: Proc 11th Int Symp Fiber Reinf Polym Reinf Concr Struct - FRPRCS-11 2013:1–7.
[40] ISO 527-2:2012. Determination of tensile properties-Part 2: Test conditions for moulding and extrusion plastics. Geneva, Switzerland; 2012.
[41] ASTM International. ASTM D3418-99: Standard Test Method for Transition Temperatures of Polymers By Differential Scanning Calorimetry. West Conshohocken, United States; 1999.
[42] ISO-11357-2. Plastics - differential scanning Calorimetry - Part 2: determi- nation of glass transition temperature. Genève, Switzerland: ISO International Organization for Standardization; 1999.
[43] Menard; KP, Menard N. Dynamic Mechanical Analysis: a practical introduction. Taylor & Francis; 2002. 10.1002/9780470027318.a2007.pub3.
[44] Borchert K, Zilch K. Bond behaviour of NSM FRP strips in service. Struct Concr 2008;9(3):127–42. https://doi.org/10.1680/stco.2007.00015.
[45] ISO International Organization for Standardization. ISO-899-1. Plastics – determination of creep behaviour – Part 1: tensile creep. Geneva, Switzerland; 2003.